

Chemical, Civil and Mechanical Engineering Tracks of 3rd Nirma University International Conference
(NUICONE 2012)

Semi-Active Control of a Benchmark Building using Neuro-Inverse Dynamics of MR Damper

Irfan H. Vadatala^a, Devesh P. Soni^b, Dolarray. G. Panchal^c

^aMtech Structures, Dharmsinh Desai University, Nadiad-387001, Gujarat, India

^bAssociate Professor, Civil Engineering Department, Sardar Vallabhbhai Patel Institute of Technology, Vasad-388 306, Gujarat, India

^cDean, Faculty of Technology, Dharmsinh Desai University, Nadiad-387001, Gujarat, India

Abstract

A six-storey benchmark problem with semi-active controller based on artificial neural network (ANN) is studied. Linear quadratic regulator (LQR) is used to generate optimal control forces. The MR damper is modeled based on parallel plate Bouc-Wen model. The combination of LQR and ANN controller is utilized to study the benchmark problem for various historical ground motions records available. It is shown that the performance of LQR and ANN is superior over the other control law for controlling the building using MR dampers.

© 2013 The Authors. Published by Elsevier Ltd. Open access under [CC BY-NC-ND license](#).

Selection and peer-review under responsibility of Institute of Technology, Nirma University, Ahmedabad.

Keywords: Bouc-Wen, Artificial neural network, Magnetorheological damper, Semi-active control.

Nomenclature

C	Damping matrix
M	Mass matrix
K	Stiffness matrix
LQR	Linear quadratic regulator
A, B, C and D	State matrices
MR	Magneto rheological
ANN	Artificial neural network
NIMR	Neuro-inverse MR Damper

1. Introduction

Earthquake forces impart energy to the structure, which produces push-pull effects to the structures causing displacements which in turn produce forces on the structure. Preliminary, response of any structure to earthquake loadings is a function of its three main inherent property, namely mass, stiffness and damping. Thus altering, adding or modifying these three properties can reduce the structural response and control the structure. Since initial conceptual studies by Yao in 1972, structural control in civil engineering has gain attention and interest resulting in research and development in the field. Structural control strategies were classified in four groups, namely passive, active, hybrid and semi-active control systems. Until about 1990, only passive control method was implemented for practical engineering systems which dissipate the earthquake energy to reduce the response. Due to limitations of passive control to become adaptable active control methods were implemented which overruled this limitation. Active control method utilizes actuators to both add and dissipate the energy. Semi-active control system combines the features of both, passive and active control strategies to reduce the responses under various earthquakes. They do not impart energy to the systems and requires very less power. Thus they

result bounded-input and bounded-output. Further semi-active devices can only produce dissipative forces. These devices include variable orifice dampers, variable friction dampers, controllable tuned liquid dampers, controllable fluid dampers etc. which can be viewed as controllable passive devices, in that the characteristics of the passive devices can be changed in real time.

Magnetorheological (MR) dampers, containing MR fluid, have been recognized as semi-active devices over the last several years. MR fluids consist of micron-sized, magnetically polarizable particles dispersed in a liquid medium such as mineral or silicone oil. MR fluids are smart, synthetic fluids changing their viscosity from liquid to semi-solid state within milliseconds if a sufficiently strong magnetic field is applied.

In the present study, artificial neural network (ANN) is trained based on inverse dynamics of MR damper to command the damper. A linear quadratic regulator (LQR) is utilized to generate the control forces. A parallel-plate MR damper model is used to represent the dynamics of MR damper. A benchmark problem presented in Jansen and Dyke [2] is selected for the study. The simulation of uncontrolled and controlled response of the building is obtained using SIMULINK [12] tool and the numerical example is tested for various ground history and the outputs are evaluated and compared.

2. Six-storey Benchmark Problem

To evaluate the applicability of ANN based on inverse dynamics of MR damper for commanding the damper, a model of six-story building equipped with four MR damper devices is considered. Two devices are rigidly connected between the ground and the first floor, and two devices are rigidly connected between the first and second floors, as shown in Fig. 1. Each MR damper is capable of producing a force equal to 30N, and the maximum voltage input to the MR devices is 5V.

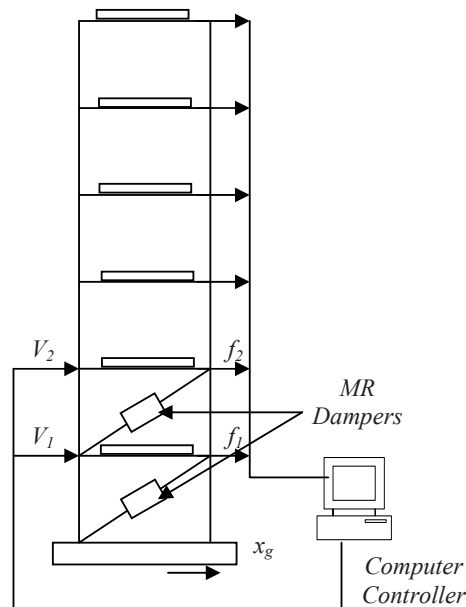


Fig. 1. Six-Storey Benchmark Problem (Jenson And Dyke [2]).

3. Control Strategy

Out of various control strategies to produce the required force, a linear quadratic regulator (LQR) is used to calculate the desire force based on the response of structure. The artificial neural network determines the required voltage based on force generated by LQR. Fig. 2 shows the schematic of the feedback control system. The measured response of the system are sensed and fed to controller which commands the MR damper to produce counter forces to dissipate the energy in the structure.

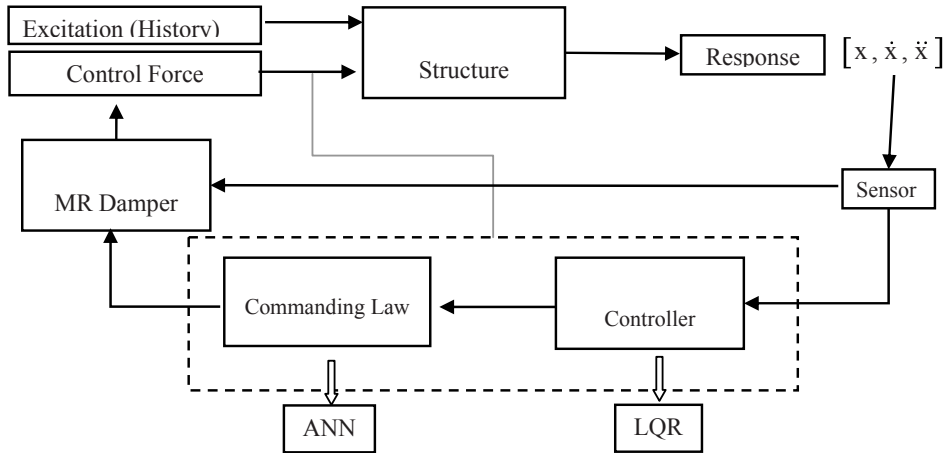


Fig. 2 Schematic of Control Strategy.

4. MR model

Due to the inherent nonlinear nature of magneto rheological dampers, one of the challenging aspects for developing and utilizing these devices to achieve high performance is the development of models that can accurately describe their unique characteristics. Although the force–displacement behavior is well represented by most of the proposed dynamic models for MR dampers, here simple Bouc-Wen model is used for the simulation due to its versatility, proposed by Jansen and Dyke[3]. Fig 3(a) shows the model followed by its governing equations.

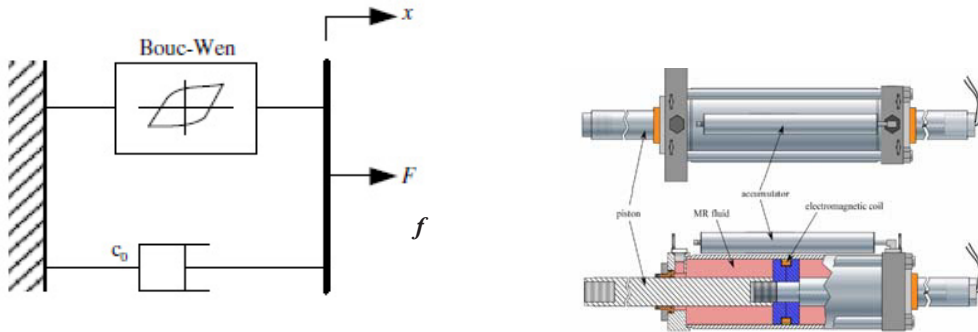


Fig. 3(a) Mechanical Model of Parallel Plate MR Dampers and Fig. 3(b) Schematic of Full Scale 20t MR Damper

$$f = c_0 \dot{x} + \alpha z \quad (1)$$

$$\dot{z} = -\gamma |\dot{x}| |z|^{n-1} - \beta \dot{x} |z|^n + A \dot{x} \quad (2)$$

$$c_0 = c_0(u) = c_{0a} + c_{0b}u \quad (3)$$

$$\alpha = \alpha(u) = \alpha_a + \alpha_b u \quad (4)$$

$$\dot{u} = -\eta (u - v) \quad (5)$$

where, z is a hysteresis component that represents a function of the time history of the displacement; A , β and γ are the shape parameters for hysteresis; n controls smoothness from pre to post yield region; α is scaling value for Bouc-Wen model; η is response time and; C_0 viscous damping. Eq.(5) is used to model the dynamics involved in reaching rheological

equilibrium and in driving the electromagnet in the MR damper (Yi et al, 1998, 1999a,b; Dyke et al., 1999). This MR damper model is used herein to model the behavior of the MR damper.

The parameters [2] selected for this model are as follows

$$\begin{aligned}\alpha_a &= 8.66 \times 10^2 \text{ N/m} \\ \alpha_b &= 8.86 \times 10^2 \text{ N/m} \\ c_{0a} &= 0.0064 \times 10^2 \text{ N.sec/m} \\ c_{0b} &= 0.0052 \times 10^2 \text{ N.sec/m} \\ A &= 120 \\ \gamma &= 300 \times 10^4 \text{ m}^{-1} \\ \beta &= 300 \times 10^4 \text{ m}^{-1} \\ \eta &= 80 \text{ sec}^{-1}\end{aligned}$$

5. System Dynamic Equations

The state matrices (A, B, C, D) can be derived as follows:

$$M\ddot{x}(t) + C\dot{x}(t) + Kx(t) = -ME\ddot{x}_g + Lu(t) \quad (6)$$

Where,

$$\begin{aligned}M &= \text{Mass matrix} \\ C &= \text{Damping matrix} \\ K &= \text{Stiffness matrix} \\ x(t) &= \text{Displacement vector of building at time } t \\ L &= \text{Location vector for control forces} \\ u(t) &= \text{Control force vector at time } t \\ E &= \text{Vector of ones} \\ \ddot{x}_g(t) &= \text{Ground accelerations at time } t\end{aligned}$$

Rewriting in state space form:

$$\dot{z}(t) = Az(t) + Bu(t) + H\ddot{x}_g(t) \quad (7)$$

$$y(t) = Cz(t) + Du(t) \quad (8)$$

The state matrices (A, B, C, D) for the uncontrolled case as shown in 5.3.1 can be derived as follows:

$$A = \begin{bmatrix} 0 & I \\ -M^{-1}K & -M^{-1}C \end{bmatrix}_{2n \times 2n} \quad B = \begin{bmatrix} 0 \\ -M^{-1}L \end{bmatrix}_{2n \times m}$$

And similarly,

$$C = \begin{bmatrix} 0 & I \\ I & 0 \\ -M^{-1}K & -M^{-1}C \end{bmatrix}_{p \times 2n} \quad D = \begin{bmatrix} 0 \\ 0 \\ -M^{-1}L \end{bmatrix}_{p \times m}$$

$$H = - \begin{bmatrix} 0 \\ E \end{bmatrix}_{2n \times 1}$$

Where m = no. of devices, n = degrees of freedom, p = no. of outputs

6. ANN controller

The MR damper model discussed earlier estimates damper forces based on the inputs of the reactive velocity and the issued voltage as described by Equations 1 to 5. The damper velocity is the same as the velocity of the floor the damper is connected to. Thus, the voltage signal is the only parameter that can be modified to control the damper force to produce the required control force. The control algorithm, LQR, estimates the required optimal control force but the MR damper force is controlled by voltage. In such case, it is essential to develop an inverse dynamic model that predicts the corresponding control voltage to be sent to the damper so that an appropriate damper force can be generated. Unfortunately, due to the inherent nonlinear nature of the MR damper, a model like that for its inverse dynamics is difficult to obtain mathematically. Because of this reason, a feed-forward back-propagation neural network is constructed to copy the inverse dynamics of the simulated MR model based on Equations 1 to 5 as suggested by Khaje-Karamodin and Haji-Kazemi [9]. This neuro-inverse model of MR Damper (NIMR) calculates the voltage signal based on the current and few previous histories of measured velocity and desirable control force. Then the voltage signals are sent to the MR damper so that it can generate the desirable optimal control forces.

6.1. Training neural network controller

Training the NIMR requires the compilation of input-output data. To completely identify the underlying MR system model, the data must contain information about the entire operating range of the system. Here, in this study, the velocity and voltage are generated randomly using band limited white Gaussian noise (WGN). WGN is a random signal with flat power spectral density (PSD) in a fixed bandwidth at any center frequency. In statistical sense it is any sequence of random variables having zero mean and a finite variance.

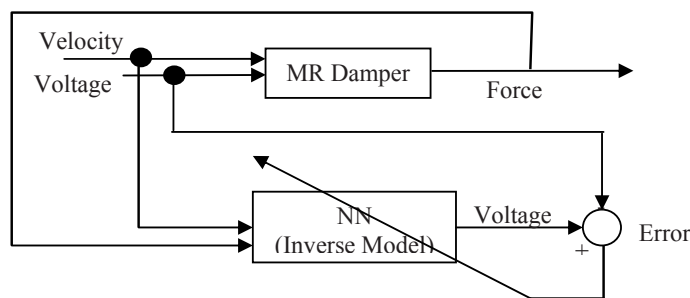


Fig. 4 Training of NIMR (Khaje-Karamodin and Haji-Kazemi [10])

The MR damper model based on Eq. (1) to (5) was used to create 6001 inputs and outputs by running the simulation for 30 sec at the sampling rate of 0.005 seconds. The numbers of inputs, outputs, hidden layers, and nodes in the hidden layers is usually done by trial and error. Also two hidden layers, each layer with ten nodes, were adopted as one of the best suitable

topologies for the NIMR The log sigmoid activation function is used for the hidden layers and the linear function for the output layer which represents the voltage. 1000 training epochs to achieve a mean-square-error (MSE) of approximately zero. The training is carried out upon the generated data using the Levenberg–Marquardt algorithm which is encoded in Neural Networks toolbox of MATLAB [12]. Fig. 4 shows feed forward back propagation training done using Levenberg-Marquardt algorithm in MATLAB.

In the present study, velocity and force are selected as input and voltage is taken as target to produce the same output after training is over with minimum error

6.2. Performance evaluation

After carrying out training, testing and validation of the trained ANN controller it was checked whether the performance of ANN controller matches with the forces produced by LQR as shown in fig. 5(a) and (b).

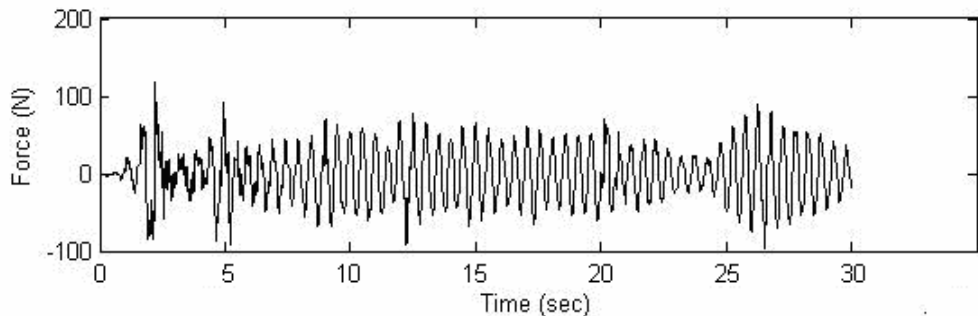


Fig. 5(a) Forces Produced by LQR

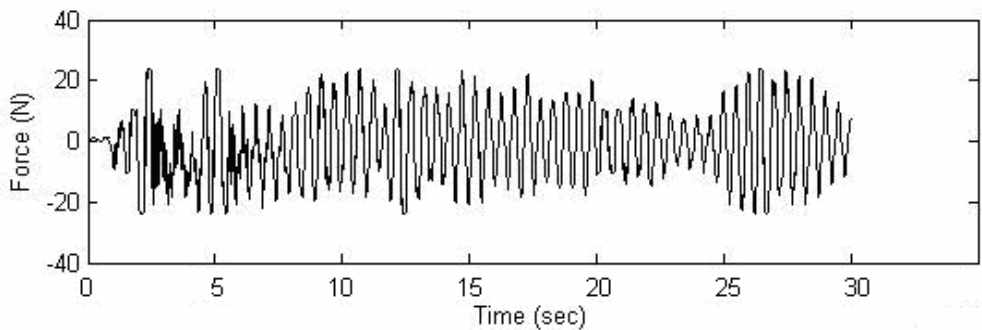
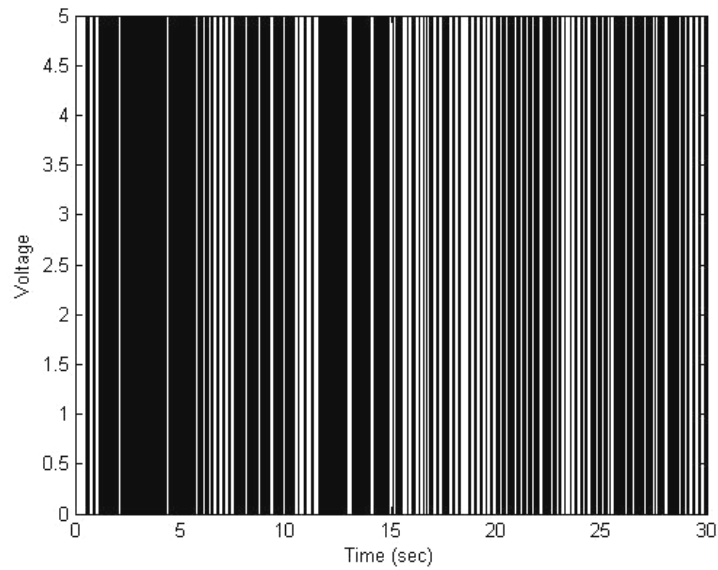
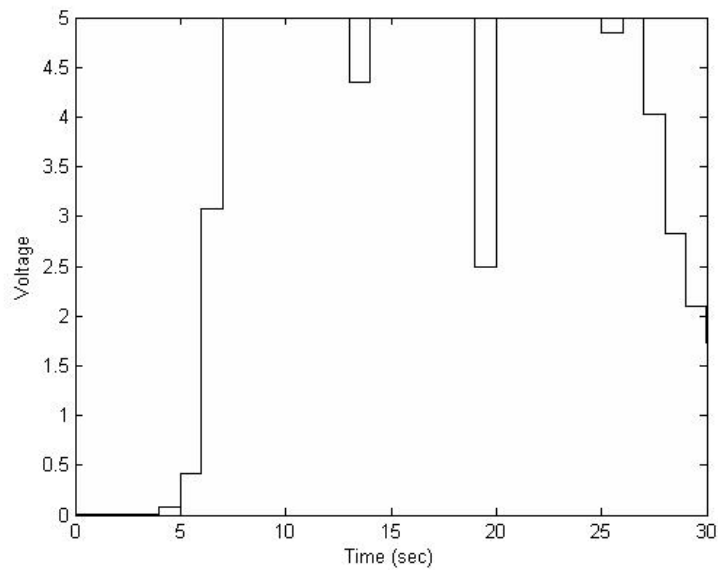


Fig. 5(b) Forces Produced by ANN

Apart from above, there has been a major advantage in using ANN controller in terms of voltage utilization. In conventional control strategy we get to use either '0' state or 'maximum stage' of voltage usage for the given system as shown in fig. 6(a). While in ANN the entire range of voltage is utilized to produce the optimal force, see fig. 6(b). Thus one can improve the efficiency of the damper and use the power available efficiently.



(a)



(b)

Fig. 6(a) Voltage Output of the Clipped optimal Controller for EL-Centro Earthquake (b) Voltage Output of the ANN Controller for EL-Centro Earthquake

The response of benchmark problem was studied under three earthquake ground motions, El-Centro (1940) with peak ground acceleration (PGA) = 0.349g, Kobe (1995) PGA = 0.82g and Northridge (1994) PGA = 0.83g. The peak responses for uncontrolled, passive-off, passive-on and ANN + LQR was compared and evaluated. Following Tables 1 to 3 shows the responses for each cases and the same are represented graphically in Fig.7 to 9.

Table 1. Peak Response Quantities of The Example Building Under Scaled El-Centro 1940 Earthquake

Control Strategy	Floor	1	2	3	4	5	6
Uncontrolled	Disp.	0.299	0.572	0.816	1.030	1.205	1.314
	Drift	0.299	0.275	0.255	0.228	0.190	0.112
	Abs acc.	52.059	79.983	92.572	92.137	103.132	147.112
Passive off	Disp.	0.239	0.450	0.673	0.869	1.032	1.133
	Drift	0.239	0.227	0.230	0.211	0.172	0.101
	Abs acc.	62.008	108.142	91.616	97.463	111.615	132.554
Passive on	Disp.	0.130	0.235	0.444	0.573	0.631	0.662
	Drift	0.130	0.106	0.212	0.177	0.149	0.116
	Abs acc.	119.798	130.208	105.547	99.325	91.804	152.615
ANN + LQR	Disp.	0.126	0.224	0.429	0.553	0.623	0.675
	Drift	0.126	0.100	0.206	0.170	0.141	0.104
	Abs acc.	125.065	132.854	110.751	92.425	109.868	136.475

Table 2. Peak Response Quantities of The Example Building Under Scaled Kobe 1995 Earthquake

Control Strategy	Floor	1	2	3	4	5	6
Uncontrolled	Disp.	1.471	2.875	4.131	5.169	5.915	6.305
	Drift	1.471	1.404	1.261	1.049	0.765	0.406
	Abs acc.	140.388	243.968	323.054	390.174	471.650	530.397
Passive off	Disp.	1.080	2.076	3.005	3.812	4.413	4.738
	Drift	1.080	1.017	0.965	0.832	0.618	0.343
	Abs acc.	174.316	279.199	267.424	318.921	414.225	448.892
Passive on	Disp.	0.342	0.642	1.006	1.343	1.589	1.718
	Drift	0.342	0.301	0.392	0.337	0.265	0.152
	Abs acc.	178.058	192.119	157.603	166.649	171.795	199.100
ANN + LQR	Disp.	0.343	0.302	0.392	0.338	0.265	0.152
	Drift	0.343	0.302	0.392	0.338	0.265	0.152
	Abs acc.	179.008	191.350	157.863	167.001	171.607	199.398

Table 3. Peak Response Quantities of The Example Building Under Scaled Northridge 1994 Earthquake

Control Strategy	Floor	1	2	3	4	5	6
Uncontrolled	Disp.	0.499	1.024	1.531	1.961	2.267	2.421
	Drift	0.499	0.528	0.508	0.431	0.306	0.155
	Abs acc.	80.370	104.601	108.037	162.948	198.892	202.442
Passive off	Disp.	0.418	0.853	1.283	1.665	1.946	2.087
	Drift	0.418	0.436	0.436	0.385	0.285	0.149
	Abs acc.	109.946	122.131	105.630	134.692	197.393	195.771
Passive on	Disp.	0.257	0.489	0.824	1.062	1.184	1.230
	Drift	0.257	0.235	0.335	0.269	0.237	0.149
	Abs acc.	182.522	139.851	157.731	154.487	163.934	194.636
ANN + LQR	Disp.	0.337	0.690	1.061	1.334	1.522	1.652
	Drift	0.337	0.355	0.375	0.300	0.257	0.137
	Abs acc.	166.729	141.832	153.065	138.024	164.932	178.768

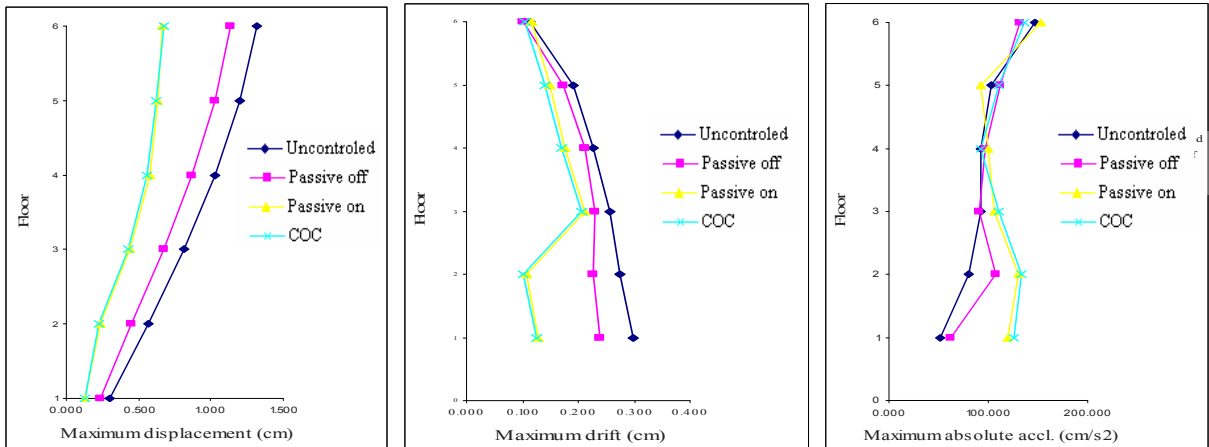


Fig. 7 Peak Responses of Each Floor of The Building To The Scaled El-Centro Earthquake

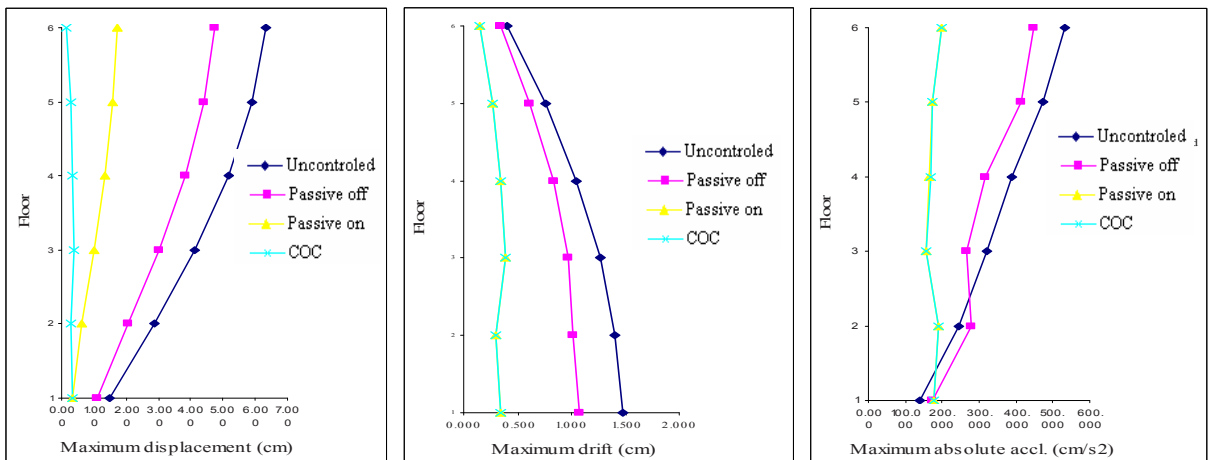


Fig. 8 Peak Responses of Each Floor of The Building To The Scaled Kobe Earthquake

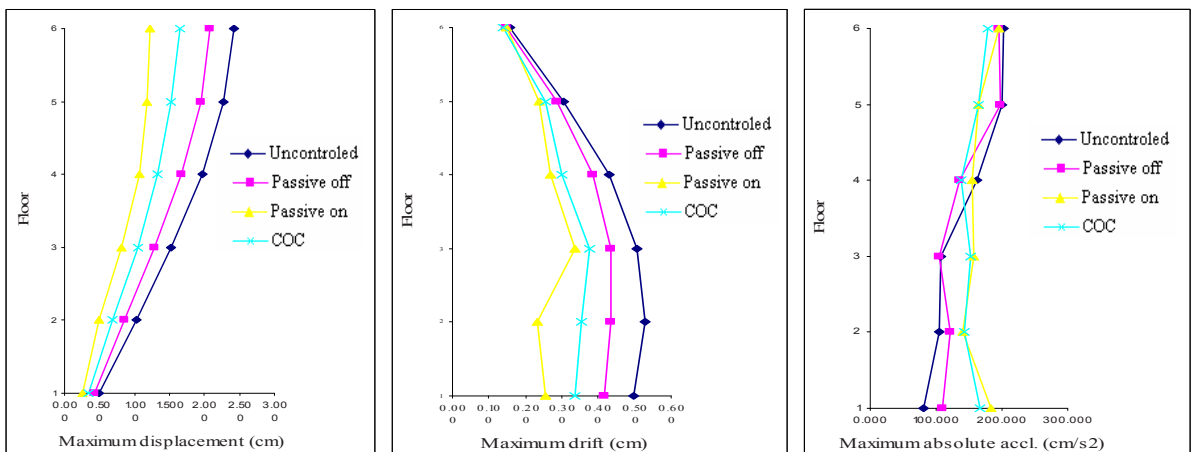


Fig. 9 Peak Responses Of Each Floor of The Building To The Scaled Northridge Earthquake

7. Summary and conclusion

Semi-active response control of a six-story building equipped with magneto rheological dampers on the lower two floors is studied. Neural network controller based on linear quadratic regulator (LQR) is employed for semi-active controller design. Parallel-plate model is utilized to investigate the nonlinear behaviour of the MR dampers. The performance of the resulting control system is compared to the uncontrolled building through simulation, and the efficiency of using MR dampers with LQR is evaluated for the selected three earthquake ground motions. The results of the study are summarized as follows.

- The passive-off system reduces the peak floor displacement, peak drift and peak absolute acceleration over the uncontrolled case.
- The passive-on system further reduces the peak floor displacement and peak drift. However, the peak absolute acceleration increases compared to the passive off system. This is due to the fact that the passive-on system attempts to lock up the first two floors, increases the drift of the upper floors and absolute acceleration of the lower floors of the building.
- The reduction in peak displacement, peak drift and peak absolute acceleration are 59%, 56% and 27%, respectively over best passive case is found using neural network controller with LQR.

References

- [1]. Chopra, A. K. (2005). "Dynamics of Structures: Theory and Application to Earthquake Engineering," New Delhi: Pearson Education.
- [2]. Jansen, L.M., Dyke. (2000). "Semi active control strategies for MR damper – A comparative study," *Journal of Engineering, Mechanics*, Vol. 126, No. 8, pp. 795–803.
- [3]. Dyke, S.J., Spencer, B.F., Sain, M. K., Carlson, J.D. (1997). "Phenomenological model of a magnetorheological damper," *Journal of Engineering, Mechanics*; Vol. 123(3):230_8.
- [4]. Dyke, S.J., Spencer, B.F. (1996). "Seismic response control using multiple MR dampers," In: 2nd international workshop on structural control. Hong Kong University of Science and Technology Research Center.
- [5]. Dyke, S.J., Spencer Jr., B.F., Sain, M.K. and Carlson, J.D. (1996). "Modeling and Control of Magnetorheological Dampers for Seismic Response Reduction," *Smart Materials and Structures*, Vol. 5, pp. 565–575.
- [6]. Dyke, S.J., Spencer Jr., B.F., Sain, M.K. and Carlson, J.D. (1997). "A Comparison of Semi-Active Control Strategies for the MR Damper," *Proc. of the IASTED Intl. Conf. on Intelligent Info. Systems*, pp. 580–584, Bahamas, December 8–10.
- [7]. Dyke, S.J., Spencer Jr., B.F., Sain, M.K. and Carlson, J.D. (1997). "An Experimental study of Magneto-rheological Dampers for Seismic Hazard Mitigation," *Proceedings of Structures Congress XV*, Portland, Oregon, U.S.A., pp. 58-62.
- [8]. Faruque Ali, Ananth Ramaswamy I. (2009). "Hybrid structural control using magnetorheological dampers for base isolated structures," *Smart Mater. Struct.* 055011 (16pp).
- [9]. Khaje-Karamodin, A., Haji-Kazemi, H. (2009). "Semi-Active Control of Structures Using a Neuro-Inverse Model of MR Damper." *Scientia Iranica* Vol. 16, No. 3. pp. 256-263.
- [10]. Kori, J.G., Jangid, R.S. (2008). "Semi active control of seismically isolated bridges," *International Journal of Structural Stability and Dynamics* Vol. 8, No. 4, pp. 547–568.
- [11]. Maryam, B., Osman, E.O. (2010). "Application of semi-active control strategies for seismic protection of buildings with MR dampers," *Engineering Structures* 32 (2010) 3040_3047.
- [12]. MATLAB, (1994). The Math Works, Inc. Natick, Mass.
- [13]. MR Dampers 2006 LORD Technical Data: RD-1005 Damper.
- [14]. Nagrath & Gopal, "Control System Engineering," New age international publication.
- [15]. Spencer, B.F., Nagarajaiah, S. "State of the Art of Structural Control,"